0026-895X/04/6606-1544–1556$20.00
MOLECULAR PHARMACOLOGY
Copyright © 2004 The American Society for Pharmacology and Experimental Therapeutics
Mol Pharmacol 66:1544–1556, 2004

Vol. 66, No. 6
2337/1182832
Printed in U.S.A.

Signaling and Ligand Binding by Recombinant Neuromedin U Receptors: Evidence for Dual Coupling to $G\alpha_{q/11}$ and $G\alpha_i$ and an Irreversible Ligand-Receptor Interaction

Paul J. Brighton, Philip G. Szekeres, Alan Wise, and Gary B. Willars

Department of Cell Physiology and Pharmacology, University of Leicester, Leicester, United Kingdom (P.J.B.; G.B.W.); and 7TMR Assay Development and Compound Profiling, GlaxoSmithKline, New Frontiers Science Park, Harlow, United Kingdom (P.G.S., A.W.)

Received May 5, 2004; accepted August 26, 2004

ABSTRACT

The neuropeptide neuromedin U (NmU) shows considerable structural conservation across species. Within the body, it is widely distributed and in mammals has been implicated in physiological roles, including the regulation of feeding, anxiety, pain, blood flow, and smooth muscle contraction. Human NmU-25 (hNmU-25) and other NmU analogs were recently identified as ligands for two human orphan G protein-coupled receptors, subsequently named hNmU-R1 and hNmU-R2. These receptors have approximately 50% amino acid homology, and, at least in mammalian species, NmU-R1 and NmU-R2 are expressed predominantly in the periphery and central nervous system, respectively. Here, we have characterized signaling mediated by hNmU-R1 and hNmU-R2 expressed as recombinant proteins in human embryonic kidney 293 cells, particularly to define their G protein coupling and the activation and regulation of signal transduction pathways. We show that these receptors couple to both $G\alpha_{q/11}$ and $G\alpha_i$. Activation of either receptor type causes a pertussis toxin-insensitive activation of both phospholipase C and mitogen activated-protein kinase and a pertussis toxin-sensitive inhibition of adenylyl cyclase with subnanomolar potency for each. Activation of phospholipase C is sustained, but despite this capacity for prolonged receptor activation, repetitive application of hNmU-25 does not cause repetitive intracellular Ca^{2+} signaling by either recombinant receptors or those expressed endogenously in isolated smooth muscle cells from rat fundus. Using several strategies, we show this to be a consequence of essentially irreversible binding of hNmU-25 to its receptors and that this is followed by ligand internalization. Despite structural differences between receptors, there were no apparent differences in their activation, coupling, or regulation.

The neuropeptide neuromedin U (NmU) was originally isolated from porcine spinal cord along with other neuromedins in the 1980s based on their ability to contract smooth muscle. Purification and characterization of NmU identified two peptides with similar biological activity (Minamino et al., 1985), both of which contracted strips of rat uterus (hence the suffix "U"). These peptides were an icosapentapeptide (NmU-25) and an octapeptide (NmU-8) identical to the C terminus of NmU-25. The search for NmU in other species identified icosapentapeptides in human (hNmU-25), rabbit, dog, frog, and chicken, a 23-amino acid version in rat and nonapeptides in guinea pig and chicken. An octapeptide has also been identified in dog, which, as with porcine NmU-8, is most likely generated through cleavage at a dibasic Arg-Arg motif present in canine and porcine NmU-25 (for review, see Brighton et al., 2004). Shorter versions of NmU are biologically active and indeed activity resides predominantly in the highly conserved C terminus. In the rat, NmU-like immunoreactivity is widely distributed with highest levels in the anterior pituitary and gastrointestinal tract (Domin et al., 1987). Significant levels are also found in the brain, spinal cord, and both the male and female genitourinary tract

This study was supported by the Biotechnology and Biological Sciences Research Council (Grant 01/A4/C/07909), the Wellcome Trust (equipment Grant 061050 for the purchase of the Ultra*VIEW* confocal microscope), and GlaxoSmithKline.

Article, publication date, and citation information can be found at http://molpharm.aspetjournals.org.

doi:10.1124/mol.104.002337.

ABBREVIATIONS: NmU, neuromedin U; NmU-R1, neuromedin U receptor 1; NmU-R2, neuromedin U receptor 2; hNmU-R1, human neuromedin U receptor 1; hNmU-R2, human neuromedin U receptor 2; hNmU-25, human neuromedin U-25; NmU-8-Cy3B, neuromedin U-8 conjugated with Cy3B; GPCR, G protein-coupled receptor; HEK, human embryonic kidney; fluo-3-AM, fluo-3-acetoxymethyl ester; $Ins(1,4,5)P_3$, inositol (1,4,5) trisphosphate; GTPγS, guanosine 5′-*O*-(3-thio)triphosphate; ERK, extracellular signal-regulated kinase; eGFP-$PH_{PLC\delta1}$, enhanced green fluorescent protein coupled to the pleckstrin homology domain of phospholipase $C_{\delta1}$; $InsP_x$ total inositol phosphates; KHB, Krebs'-based HEPES buffer; pERK, phospho-extracellular signal-regulated kinase; MAP, mitogen-activated protein.

(Domin et al., 1986). Circulating NmU has not been detected, suggesting that it acts as a neuropeptide or neuromodulator rather than as a circulating hormone (Augood et al., 1988).

Despite an appreciation of the tissue distribution of NmU in several species and a detailed understanding of structure-activity relationships, its physiological roles remain to be defined precisely. NmU contracts smooth muscle in a tissue- and species-specific manner (Minamino et al., 1985; Bockman et al., 1989; Maggi et al., 1990; Westfall et al., 2001), regulates regional blood flow and blood pressure (Gardiner et al., 1990), and influences the pituitary-adrenal-cortical axis (Malendowicz et al., 1993). Intracerebroventricular administration of NmU mediates stress responses and increases both arterial pressure and heart rate in conscious rats (Westfall et al., 2001; Chu et al., 2002), indicating a role in the regulation of sympathetic nervous activity and cardiovascular function. In rats, intracerebroventricular injection of NmU also decreases food intake and body weight (Howard et al., 2000; Kojima et al., 2000; Nakazato et al., 2000; Ivanov et al., 2002; Wren et al., 2002) and increases gross locomotor activity, body temperature, heat production, and oxygen consumption (Howard et al., 2000; Nakazato et al., 2000). Interestingly leptin evokes the release of NmU from hypothalamic explants (Wren et al., 2002), suggesting that the effects of leptin on feeding, body weight, and metabolism may also be mediated, at least in part, through NmU.

The recent identification of a human orphan G protein-coupled receptor (GPCR) as a specific target for NmU (human neuromedin U-receptor 1; hNmU-R1) (Fujii et al., 2000; Hedrick et al., 2000; Hosoya et al., 2000; Howard et al., 2000; Kojima et al., 2000; Raddatz et al., 2000; Shan et al., 2000; Szekeres et al., 2000) and the subsequent identification of an additional receptor (human neuromedin U-receptor 2; hNmU-R2) (Hosoya et al., 2000; Howard et al., 2000; Raddatz et al., 2000; Shan et al., 2000) has greatly enhanced interest and understanding of NmU. Both receptors show characteristics of family 1 GPCRs and have approximately 50% amino acid homology. Recombinant NmU receptors elevate intracellular $[Ca^{2+}]$ ($[Ca^{2+}]_i$) with nanomolar potency (Fujii et al., 2000; Hedrick et al., 2000; Hosoya et al., 2000; Howard et al., 2000; Kojima et al., 2000; Raddatz et al., 2000; Shan et al., 2000; Szekeres et al., 2000; Funes et al., 2002) although it is unclear whether they couple to other signaling pathways (Hosoya et al., 2000; Szekeres et al., 2000). The distribution of mRNA suggests that NmU-R1 and NmU-R2 are located predominantly but not exclusively in peripheral tissues and the central nervous system, respectively (Hedrick et al., 2000; Hosoya et al., 2000; Howard et al., 2000; Raddatz et al., 2000; Shan et al., 2000; Szekeres et al., 2000; Westfall et al., 2001). These distribution patterns have started to allow the assignment of particular physiological roles to the receptor subtypes. However, overlapping expression and the absence of selective ligands has made it difficult to define which receptors mediate specific responses and which intracellular signaling pathways are involved. The discovery of receptors for NmU presents the possibility of characterizing the cellular signaling pathways regulated by NmU. In the current study, we have explored the signaling mediated by recombinantly expressed NmU receptors, examining their coupling to intracellular signal transduction pathways, desensitization profiles, and potential differences between the receptor subtypes.

Materials and Methods

Materials

HEK293 cell culture reagents were from Invitrogen (Paisley, UK), and primary cell culture reagents were supplied by Cascade Biologics (Nottingham, UK). Cell culture plastic-ware was from NUNC A/S (Roskilde, Denmark). Fluo-3-acetoxymethyl ester (fluo-3-AM) was supplied by TEF Labs (Austin, TX) and fluo-4-AM and Pluronic F-127 were from Molecular Probes (Leiden, The Netherlands). [*myo*-^{3}H]Inositol (71 Ci/mmol) and ^{125}I-hNmU-25 (2000 Ci/mmol) were from Amersham Biosciences UK, Ltd. (Little Chalfont, Buckinghamshire, UK); [^{3}H]inositol 1,4,5-trisphosphate ([^{3}H]Ins(1,4,5)P_3) (22 Ci/mmol), [^{3}H]cAMP (34 Ci/mmol), and [^{35}S]GTPγS (1250 Ci/mmol) were from PerkinElmer Life and Analytical Sciences (Boston, MA). Biocoat 384-well black-walled clear-bottomed microtiter plates were from BD Biosciences (Bedford, MA). Costar polypropylene 96-well plates, Unifilter 96-well white microplates with bonded Whatman GF/B filters, and Microscint 20 scintillation fluid were all supplied by PerkinElmer Life and Analytical Sciences (Boston, MA). Emulsifier-safe scintillation fluid was supplied by Packard Bioscience (Groningen, The Netherlands). Protein A-Sepharose beads were supplied by Amersham Biosciences (Uppsala, Sweden) and nitrocellulose membrane (Protran) was supplied by Schleicher & Schuell (Keene, NH). The monoclonal antibody specific for $G\alpha_{q/11}$ (Bundey and Nahorski, 2001) was generated by Genosys Biotechnologies (Pampisford, UK) by inoculation of rabbits with the common C-terminal (positions 344–353) sequence (C)QLNLKEYNLV. Antibodies against $G\alpha_{i(1-3)}$ (SC-410) and $G\alpha_s$ (SC-823), ERK (SC-93), and phospho-ERK (SC-7383) were from Santa Cruz Biotechnology, Inc. (Santa Cruz, CA). The enhanced chemiluminescence Western blotting system was from Amersham Biosciences UK, Ltd. The transfection reagents Genejuice and LipofectAMINE Plus were from Novagen (Madison, WI) and Invitrogen, respectively. Protease inhibitor cocktail set 1 was from Calbiochem (Nottingham, UK). hNmU-25 was made at GlaxoSmithKline (Harlow, UK).

Other reagents were supplied by either Sigma Chemical (Poole, Dorset, UK), Fisher Scientific (Loughborough, UK), Merck (Darmstadt, Germany), or BDH Laboratory Supplies (Poole, Dorset, UK).

Cell Culture and Creation of Stable Cell Lines Expressing hNmU-R1 or hNmU-R2

HEK293 cells were maintained in minimal essential medium with Earl's salts supplemented with 10% fetal calf serum, nonessential amino acids, and 50 μg/ml gentamycin. Cells were maintained in 175-cm^2 flasks at 37°C in a 95%/5% air/CO_2-humidified environment. Cells for experimental use in multiwell plates or on coverslips were cultured on poly-D-lysine-coated surfaces. The DNA encoding hNmU-R1 was cloned into EcoR1/EcoRV and hNmU-R2 into Asp718/BamHI of pCDN (Aiyar et al., 1994). Constructs were transfected using LipofectAMINE Plus and grown under selection (400 μg/ml Geneticin). Clonal cell lines were expanded from single foci and screened by determination of hNmU-25-mediated elevation of $[Ca^{2+}]_i$ in fluo-3-AM-loaded cells using a fluorescence imaging plate reader (FLIPR), accumulation of total inositol phosphates ([^{3}H]InsP_x), and Ins(1,4,5)P_3 production using both single cell and population assays (see below). Relative expression levels were examined by the binding of ^{125}I-hNmU-25 to membrane preparations using a concentration of ligand approximating to the K_d (see below). Single clones expressing either hNmU-R1 or hNmU-R2 were selected based on both similar expression levels and approximately equivalent functional responses mediated by hNmU-25 (10 nM).

Dissociation and Culture of Rat Stomach Fundus Smooth Muscle Cells

Cells were isolated by enzyme digestion and mechanical sheering of diced fundus from adult male Wistar rats (<300 g) using a protocol originally optimized for the dissociation of pig coronary artery

smooth muscle cells (Quayle et al., 1996). Animals were handled in accordance with the UK Animals (Scientific Procedures) Act, 1986. After collection of cells by centrifugation (500*g*; 3 min), they were resuspended and cultured (37°C; 5% CO_2) on untreated 25-mm glass coverslips in medium 231 supplemented with 5% smooth muscle growth supplement, 50 μg/ml streptomycin, 50 IU/ml penicillin, and 50 μg/ml gentamycin.

Binding of ^{125}I-hNmU-25

Membrane Preparation. Confluent cell monolayers were harvested with phosphate-buffered saline, collected by centrifugation (200*g*; 2 min; 4°C), and resuspended in homogenization buffer (composition 1 mM EDTA, 10 mM Tris-HCl, 1 mM phenylmethylsulfonyl fluoride, and 200 μg/ml benzamidine, pH 7.4). After 15 min on ice, cells were homogenized and centrifuged (20,000*g*; 4°C; 10 min), and the pellets were resuspended in homogenization buffer at 1 mg/ml protein.

^{125}I-hNmU-25 Saturation Binding. Experiments were performed in buffer (composition, unless otherwise stated, 20 mM Tris-HCl, pH 7.4, 5 mM $MgCl_2$, 2 mM Na-EGTA, and 0.1 mg/ml bacitracin) in 100-μl volumes in a 96-well format using 10 μg of membrane and ^{125}I-hNmU-25 at 0.1 to 1000 pM. Nonspecific binding was determined using 1 μM hNmU-25 with a 5-min preincubation period. After 1 h at room temperature, 100 μl of ice-cold 0.9% NaCl was added, and the suspension was rapidly filtered through 0.3% polyethylenimine presoaked Unifilter 96-well microplates with bonded Whatman GF/B filters. Recovered radioactivity was determined by standard liquid scintillation counting.

Determination of G Protein Activation

Membrane Preparation. Cells were harvested with phosphate-buffered saline, collected by centrifugation (200*g*; 5 min; 4°C), and the pellet was homogenized in lysis buffer (composition 10 mM HEPES and 10 mM EDTA, pH 7.4). This suspension was centrifuged (30,000*g*; 15 min; 4°C), and the final pellet was homogenized in freezing buffer (composition 10 mM HEPES and 0.1 mM EDTA, pH 7.4). Protein concentration was adjusted to 1 mg/ml.

[^{35}S]GTPγS Binding and Immunoprecipitation of Gα-Subunits. Determination of G protein activation was by [^{35}S]GTPγS binding and immunoprecipitation of specific Gα-subunits (Akam et al., 2001) using membranes (25 μg) incubated with either 1 μM (for $G\alpha_{q/11}$) or 10 μM (for $G\alpha_i$ and $G\alpha_s$) GDP and 1 nM [^{35}S]GTPγS. Where appropriate, tubes contained 10 μM GTPγS to determine nonspecific binding and/or 10 nM hNmU-25. After incubation (2 min; 37°C), the reaction was terminated with ice-cold buffer, and membranes were pelleted by centrifugation. Pellets were solubilized, precleared, and incubated overnight at 4°C with 5 μl of Gα-specific antisera (1:100 dilution). Immune complexes were isolated with protein A-Sepharose beads, collected by centrifugation, and extensively washed. Beads were resuspended in scintillation fluid and ^{35}S was determined.

Determination of Phospholipase C Activity

Total [^{3}H]InsP_x Accumulation. Cell monolayers in 24-well plates were loaded with 3 μCi/ml of [*myo*-^{3}H]inositol for 48 h, and, if required, treated with 100 ng/ml pertussis toxin for the last 20 to 24 h. Cells were washed twice with 1 ml of Krebs'-based HEPES buffer (KHB) [composition, unless otherwise stated, 10 mM HEPES, 4.2 mM $NaHCO_3$, 11.7 mM D-glucose, 1.18 mM $MgSO_4 \cdot 7H_2O$, 1.18 mM KH_2PO_4, 4.69 mM KCl, 118 mM NaCl, 1.29 mM $CaCl_2 \cdot 2H_2O$, and 0.01% (w/v) bovine serum albumin, pH 7.4] and equilibrated at 37°C for 15 min with 250 μl of KHB containing 10 mM LiCl. For experiments here and elsewhere, Ca^{2+}-free conditions were obtained by the exclusion of $CaCl_2 \cdot 2H_2O$ from the KHB. Cells were challenged with agonist, and the reaction was terminated with an equal volume of ice-cold, 1 M trichloroacetic acid. [^{3}H]InsP_x were extracted and separated by anion exchange chromatography (Willars and Nahorski, 1995).

Ins(1,4,5)P_3 Mass Generation. Cell monolayers in 24-well plates were washed with 1 ml of KHB and incubated at 37°C for 10 min with 200 μl of KHB. Cells were challenged with 50 μl of KHB containing hNmU-25 as required. Reactions were terminated by the addition of an equal volume of 1 M trichloroacetic acid. Ins(1,4,5)P_3 was extracted and determined using a radioreceptor assay (Willars and Nahorski, 1995) and related to cell protein content.

Single Cell Imaging of Phospholipase C Activity. The vector containing the fusion construct between the enhanced green fluorescent protein and the pleckstrin homology domain of phospholipase $C_{\delta 1}$ (eGFP-$PH_{PLC\delta 1}$) was generously provided by Professor T. Meyer (Stanford University, Stanford, CA) and used to monitor phospholipase C activity in single cells as described previously (Nash et al., 2001). In brief, cells on 25-mm coverslips were transfected with 1 μg of eGFP-$PH_{PLC\delta 1}$ plasmid cDNA using Genejuice transfection reagent. Cells were cultured for 48 h, and coverslips were mounted onto the stage of an Ultra*VIEW* confocal microscope (PerkinElmer Life and Analytical Sciences, Cambridge, UK) with a 40× oil emersion objective and excited at 488 nm using a Kr/Ar laser. Emitted light was collected above 510 nm, and images were captured at approximately 1 s^{-1}. The chamber volume was maintained at approximately 0.5 ml and perfused (5 ml/min) with KHB heated to 37°C with a Peltier unit. When cells were initially exposed to hNmU-25, perfusion was stopped, and additions were made directly to the cell chamber. Cytosolic fluorescence provides an index of Ins(1,4,5)P_3 levels and is expressed as the change in fluorescence relative to that in the 30 s preceding agonist application.

Determination of $[Ca^{2+}]_i$

Confocal $[Ca^{2+}]_i$ Imaging. Changes in $[Ca^{2+}]_i$ in single cells were performed essentially as described previously (Werry et al., 2002). In brief, cells on 25-mm coverslips were loaded with 5 μM fluo-3-AM with 0.044% (w/v) Pluronic F-127 for 1 h (HEK293 cells) or 30 min (rat fundus smooth muscle cells) at room temperature and imaged as described above. Addition of hNmU-25 and thapsigargin was by bath application in the absence of perfusion. Other agonists and changes in buffer were via perfusion of the chamber (see above). Cytosolic fluorescence provides an index of the $[Ca^{2+}]_i$ and is expressed as the change in fluorescence relative to that in the 30 s preceding agonist application.

FLIPR Analysis. Cells were seeded into 384-well microtiter plates at 10,000 cells $well^{-1}$ and cultured for 24 h. Cell counts were achieved by counting particles of 9.5 to 30 μm with a Beckman Coulter Z-series cell counter (Beckman Coulter, High Wycombe, Buckinghamshire, UK). After loading (1 μM fluo-4-AM in KHB for 1 h at 37°C), cells were washed three times and incubated for 10 min before assay on an FLIPR at 37°C. The response after agonist addition was taken as the maximum fluorescence intensity units less the minimum immediately before addition.

Inhibition of Forskolin-Induced cAMP Accumulation

Cell monolayers in 24-well plates were washed with 1 ml of KHB and incubated at 37°C for 10 min with 1 ml of KHB. Buffer was aspirated and replaced by 200 μl of buffer containing agonist at the required concentration. After a 10-min incubation at 37°C, a further 50 μl of buffer containing both agonist at the required concentration and forskolin (final concentration 10 μM) was added. After a further 10-min incubation at 37°C, buffer was removed and reactions were terminated with ice-cold 0.5 M trichloroacetic acid. The cAMP was extracted using a method identical to that for the extraction of Ins(1,4,5)P_3 (Willars and Nahorski, 1995). The cAMP content was determined using a radioreceptor assay with binding protein purified from calf adrenal glands (Brown et al., 1971) and related to cellular protein levels.

Determination of ERK Activation

Receptor Activation and Cell Solubilization. Cells on 24-well plates were washed and equilibrated in KHB at 37°C. Cells were stimulated with 10 nM hNmU-25 at 37°C, and reactions were terminated by aspiration and addition of ice-cold solubilization buffer [composition, unless otherwise stated, 100 mM Tris, 10 mM EDTA, 150 mM NaCl, 1% Nonidet P-40 (v/v), 0.1% SDS, 5 mg/ml deoxycholic acid, 200 μg/ml benzamidine, 1 mM phenylmethylsulfonyl fluoride, and protease inhibitor cocktail, pH 7.4]. Cell lysates were precleared by centrifugation (12,000*g*; 10 min; 4°C), and supernatant was adjusted to 3 mg/ml protein.

Western Blotting. Proteins (30 μg) were separated by 10% SDS-PAGE, transferred onto nitrocellulose membranes, blocked, and probed for ERK. Blots were then stripped and reprobed for phospho-ERK (pERK). In each case, visualization was achieved using horseradish peroxidase-conjugated secondary antibodies, enhanced chemiluminescence detection, and autoradiography. Densitometric analysis of the autoradiographs was achieved with a Syngene (Cambridge, UK) Bio Imaging System using Genesnap-GeneGnome software (Syngene) using only the density of p38 ERK (ERK 1) against which the antibody was raised.

Generation of Fluorescently Tagged Porcine NmU-8 and Binding to Cells Expressing Either hNmU-R1 or hNmU-R2

Generation of NmU-8-Cy3B. Cy3B was attached to the N terminus of porcine NmU-8 using Cy3B-NHS ester (Amersham Biosciences UK, Ltd.), following standard conditions as recommended by the manufacturer. The product (NmU-8-Cy3B) was purified by C18 reverse-phase high-performance liquid chromatography, and mass was confirmed by matrix-assisted laser desorption ionization.

Imaging of NmU-8-Cy3B. Cells were seeded onto 25-mm-diameter poly-D-lysine-coated glass coverslips and cultured for 24 to 48 h. Cells were washed with KHB, and the coverslips were mounted onto the stage of an Ultra*VIEW* confocal microscope. Cells were excited at 568 nm using a krypton/argon laser, and emitted light was collected with a broad band RGB emission filter. NmU-8-Cy3B was added via bath application at a concentration of 10 nM, and images were taken at a rate of approximately 1 s^{-1}. Where appropriate, KHB was perfused over the cells at a rate of 5 ml/min. Temperature was controlled at 37°C with a Peltier unit, or at 12°C with a Peltier unit and perfusion of ice-cold buffer.

Data Analysis

Concentration-response curves and saturation radioligand binding data were fitted using Prism (GraphPad Software Inc., San Diego, CA) using a standard four-parameter logistic equation. All data shown are expressed as the mean of three experiments (unless otherwise stated) ± S.E.M. For representative data, experiments were also performed to an n of three or more.

Results

Expression of Recombinant hNmU-R1 and hNmU-R2. The binding of ^{125}I-hNmU-25 to membranes from the clonal cell lines expressing either hNmU-R1 or hNmU-R2 was saturable with the nonspecific component representing approximately 50% of the total at saturating concentrations of ^{125}I-hNmU-25. There was no specific binding to wild-type (nontransfected) HEK293 cells (data not shown). Saturation binding curves indicated B_{max} values of 4.88 ± 0.33 and 1.95 ± 0.16 pmol/mg for hNmU-R1 and hNmU-R2, respectively. These experiments also indicated K_d values of $-9.87 \pm 0.05 \log_{10}$ M (135 pM) and $-9.95 \pm 0.10 \log_{10}$ M (112 pM) for hNmU-R1 and hNmU-R2, respectively. However, it must be noted that given the characteristics of NmU binding that indicate a lack of reversibility (see below), these K_d values may be of limited value in describing the binding characteristics.

G Protein Coupling of hNmU-R1 and hNmU-R2 in Cell Membranes. Binding of [^{35}S]GTPγS to immunoprecipitated $G\alpha_{q/11}$ (Fig. 1a) or $G\alpha_{i(1-3)}$ (Fig. 1c) increased by approximately 3-fold over basal upon activation of either hNmU-R1 or hNmU-R2 with 10 nM hNmU-25. The binding of [^{35}S]GTPγS to $G\alpha_s$ did not increase after activation of either receptor type (Fig. 1b), although activation of endogenously expressed β_2-adrenoceptors with 100 μM noradrenaline resulted in an approximately 1.5–2 fold increase above basal levels (data not shown). Nonspecific binding using 10 μM GTPγS was ~20 to 50% of basal (unstimulated) [^{35}S]GTPγS binding (Fig. 1). In additional cell lines expressing either hNmU-R1 or hNmU-R2 at 26 and 31%, respec-

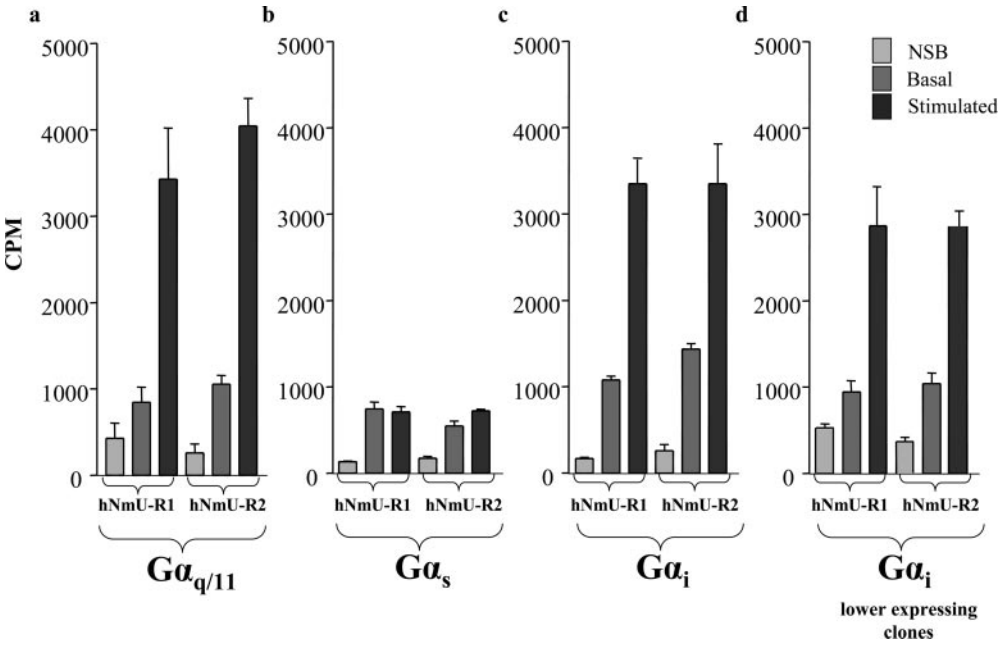

Fig. 1. G protein coupling of hNmU-R1 and hNmU-R2. Membrane preparations (25 μg) from cells expressing either hNmU-R1 or hNmU-R2 were incubated in the presence of GDP [1 μM for $G\alpha_{q/11}$ and 10 μM for $G\alpha_{i(1-3)}$ and $G\alpha_s$], 1 nM [^{35}S]GTPγS, and where applicable hNmU-25 (10 nM) (Stimulated). Nonspecific binding (NSB) was determined using 10 μM GTPγS. Immunoprecipitation was carried out using antibodies against specific Gα subunits as indicated, and associated [^{35}S] was determined. The binding of [^{35}S]GTPγS to $G\alpha_{i(1-3)}$ subunits using membranes prepared from additional lower expressing clones is also shown (d). All data are mean + S.E.M., n = 4.

tively, of the level in cells used throughout the rest of the study (data not shown), 10 nM NmU also increased [^{35}S]GTPγS binding to $G\alpha_{i(1-3)}$ by approximately 2.5- to 3-fold over basal (Fig. 1d).

hNmU-25-Mediated Phosphoinositide Signaling. In cells expressing either hNmU-R1 or hNmU-R2, 10 nM hNmU-25 caused marked accumulations of [^{3}H]InsP_x against a Li^+ block of inositol monophosphatase activity (Fig. 2a) that continued until the furthest time tested (60 min). Accumulation was biphasic, with a rapid phase (300–350% over basal/min) that became (at ~20 s) slower (50–60% over basal/min) but sustained (Fig. 2b), suggesting a rapid but partial desensitization of phospholipase C activity. Challenge of wild-type HEK293 cells with 10 nM hNmU-25 did not result in accumulation of [^{3}H]InsP_x (data not shown). The accumulation of [^{3}H]InsP_x was concentration-dependent, with similar pEC_{50} values of 9.14 ± 0.07 and 8.97 ± 0.18 for hNmU-R1 or hNmU-R2, respectively (Fig. 2, c and d). Pertussis toxin had no effect on hNmU-25-mediated accumulation of [^{3}H]InsP_x in either cell line (Fig. 2, c and d), indicating a lack of involvement of $G\alpha_{i/o}$ in NmU-mediated phospholipase C responses. In cells expressing hNmU-R1, challenge with 10 nM hNmU-25 in the absence of extracellular Ca^{2+} had no effect on the biphasic profile of the accumulation of [^{3}H]InsP_x, but by 60 min it had reduced the accumulation to 40 ± 10% (n = 3) of that seen in the presence of extracellular Ca^{2+}.

Activation of either receptor type with 10 nM hNmU-25 resulted in a rapid and marked increase in Ins(1,4,5)P_3 mass that peaked at 10 s and declined to a lower but sustained phase (Fig. 3a).

Transfection of cells expressing either hNmU-R1 or hNmU-R2 with eGFP-$PH_{PLC\delta\ 1}$ resulted in the expression of the construct and localization predominantly to the plasma membrane (Fig. 3, b and c, A) because of the high affinity of the pleckstrin homology domain for PtdIns(4,5)P_2. Activation of either hNmU-R1 or hNmU-R2 with 10 nM hNmU-25 resulted in the translocation of eGFP-$PH_{PLC\delta1}$ to the cytosol followed by a partial relocalization to the plasma membrane (Fig. 3, b and c, B and C). This was reflected in analysis of cytosolic fluorescence intensity (Fig. 3, b and c). Translocation to the cytosol is a consequence of the higher affinity of eGFP-$PH_{PLC\delta1}$ for Ins(1,4,5)P_3 than PtdIns(4,5)P_2 and therefore reflects cellular levels of Ins(1,4,5)P_3 (Nash et al., 2001).

hNmU-25-Mediated Ca^{2+} Signaling. Single cell imaging of $[Ca^{2+}]_i$ in cells expressing either hNmU receptor revealed robust (2–3-fold over basal), rapid (5-s) peaks followed by lower (1.2–1.4-fold over basal) sustained phases in response to 10 nM hNmU-25 (Fig. 4, a and b). Removal of extracellular Ca^{2+} had little effect on the peak elevation but abolished the sustained phase (data not shown). Removal of extracellular Ca^{2+} during the hNmU-25-mediated sustained elevation of $[Ca^{2+}]_i$ caused a reduction in $[Ca^{2+}]_i$ back to basal levels in hNmU-R1 and hNmU-R2 cell lines (data not shown). Pretreatment of cells for 10min with the sarco/endoplasmic reticulum Ca^{2+}-ATPase inhibitor thapsigargin (1 μM) abolished the Ca^{2+} responses in both hNmU-R1 and hNmU-R2 expressing cells (data not shown).

Analysis of Ca^{2+} signaling by FLIPR demonstrated hNmU-25-mediated $[Ca^{2+}]_i$ profiles in populations consistent with those in single cells (Fig. 4, c and d). The pEC_{50} values for the hNmU-25-mediated peak elevation of $[Ca^{2+}]_i$ in hNmU-R1 and hNmU-R2 cells were 9.41 ± 0.09 and 9.37 ± 0.06, respectively (Fig. 4, e and f).

hNmU-25-Mediated Regulation of cAMP. Activation of either hNmU-R1 or hNmU-R2 with hNmU-25 resulted in the inhibition of forskolin (10 μM)-stimulated cAMP accumulation (Fig. 5) with pEC_{50} values of 10.10 ± 0.16 and 10.06 ± 0.17 in cells expressing hNmU-R1 or hNmU-R2, respectively. Pertussis-toxin treatment (20 h; 100 ng/ml) abolished this inhibition of forskolin-stimulated cAMP accumulation (Fig. 5). Addition of 10 nM hNmU-25 did not increase cAMP in

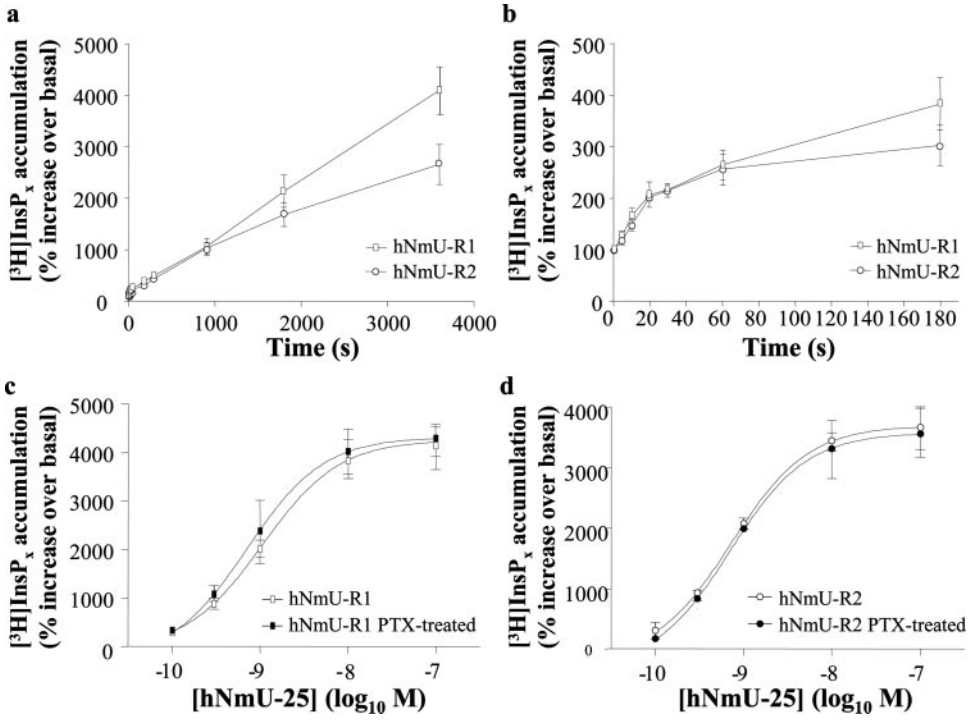

Fig. 2. hNmU-R1- and hNmU-R2-mediated accumulation of [^{3}H]InsP_x. Cells expressing either hNmU-R1 (□) or hNmU-R2 (○) were seeded into 24-well plates and loaded with [*myo*-^{3}H]inositol for 48 h. a, cells were challenged with 10 nM hNmU-25 for varying lengths of time ranging from 0 to 3600 s (60 min) in the presence of a 10 mM Li^+ block of inositol monophosphatase activity. b, detail from a showing the accumulation of [^{3}H]InsP_x over the first 180 s of agonist stimulation. Concentration-response curves for the accumulation of [^{3}H]InsP_x after activation of either hNmU-R1 (c) or hNmU-R2 (d) by hNmU-25. Cells were challenged under Li^+ block for 60 min. The pEC_{50} values were 9.14 ± 0.07 and 8.97 ± 0.18 for hNmU-R1 and hNmU-R2, respectively. Where applicable, cells were treated with 100 ng/ml pertussis toxin (PTX) for 24 h before agonist challenge (filled symbols). [^{3}H]InsP_x accumulations are presented as the percentage of increase relative to basal levels. Data are mean ± S.E.M., n = 3.

cells expressing either receptor in the presence or absence of the phosphodiesterase inhibitor 3-isobutyl-1-methylxanthine (500 μM) (data not shown). In contrast, challenge of endogenously expressed $G\alpha_s$-coupled β_2-adrenoceptors caused a 5-fold increase in cAMP above basal levels in the absence of 3-isobutyl-1-methylxanthine (data not shown).

Activation of ERK by hNmU-R1 and hNmU-R2. Challenge of either hNmU-R1 (Fig. 6a, i) or hNmU-R2 (Fig. 6b, i) with 10 nM hNmU-25 did not alter cellular levels of ERK. However, hNmU-25 increased the level of pERK, which peaked after 5 to 10 min of stimulation and then slowly declined (Fig. 6a, ii; b, ii; and c). ERK phosphorylation after activation of either receptor subtype was unaffected by pertussis toxin (24 h; 100 ng/ml; data not shown).

Desensitization of hNmU-R and Irreversible Binding of hNmU-25 under Physiological Conditions. Single cell $[Ca^{2+}]_i$ imaging demonstrated that after the stimulation of either hNmU-R1- or hNmU-R2-expressing cells with 10 nM hNmU-25, perfusion with agonist-free buffer did not return the $[Ca^{2+}]_i$ to basal levels. Furthermore, reapplication of 10 nM hNmU-25 after this perfusion had no effect on $[Ca^{2+}]_i$ (Fig. 7, a and b). Application of 100 μM carbachol to activate endogenous $G\alpha_{q/11}$-coupled muscarinic M_3 receptors also evoked a peak and plateau of $[Ca^{2+}]_i$ elevation that was similar to that evoked by 10 nM hNmU-25 (Fig. 7c). Subsequent perfusion of agonist-free buffer reduced $[Ca^{2+}]_i$ to basal levels, and reapplication of 100 μM carbachol resulted in a Ca^{2+} response that was 40 $\pm$ 10% (n = 34 cells) of the original (Fig. 7c). In hNmU-R1-expressing cells, the addition of 10 nM hNmU-25 at 150 s after 100 μM carbachol resulted in a Ca^{2+} response of approximately 50 $\pm$ 10% (n = 26 cells) of that achieved by the addition of hNmU-25 to naive cells (n = 26 cells). However, if cells were washed (120 s) with agonist-free buffer after 100 μM carbachol and then 10 nM, hNmU-25 evoked a Ca^{2+} response that was 105 $\pm$ 15% (n = 45 cells) of that induced by addition of 10 nM hNmU-25 to naive cells. In contrast, application of 100 μM carbachol at 150 s after hNmU-25 evoked a Ca^{2+} response that was only approximately 25% that of the initial hNmU-25 response, irrespective of whether there had been a wash period (120 s) or not after hNmU-25 application (n = 37 and 47 cells, respectively) (data not shown).

In primary isolates of rat fundus, individual smooth muscle cells that had been allowed to adhere to coverslips for several hours often showed robust contractions to stimulation with either 300 μM UTP or 10 nM hNmU-25 (data not shown). These contractions most often resulted in cell rounding and detachment from the coverslip. Cells that had been cultured for 5 to 7 days were more firmly adhered to the coverslip, and robust contractions were rarely seen. However, in cells loaded with fluo-3 and imaged by confocal microscopy, either 300 μM UTP (Fig. 8a) or 10 nM hNmU-25 (Fig. 8b) evoked marked peak and plateau elevations of $[Ca^{2+}]_i$. Perfusion with agonist-free buffer reduced $[Ca^{2+}]_i$ to basal levels after stimulation with UTP (Fig. 8c) but not hNmU-25 (Fig. 8d). Furthermore, after this wash period (120 s), reapplication of UTP (Fig. 8c) but not hNmU-25 (Fig. 8d) resulted in a further elevation of $[Ca^{2+}]_i$.

After hNmU-25, the inability of a wash with buffer to fully restore subsequent Ca^{2+} responses to either hNmU-25 or car-

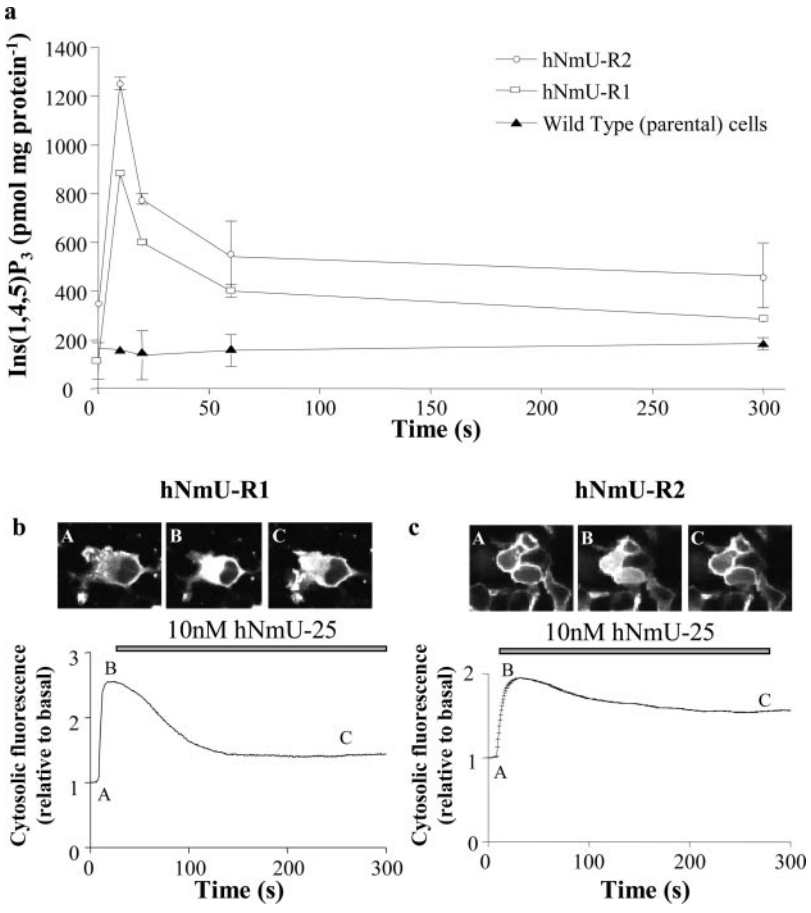

Fig. 3. hNmU-R1- and hNmU-R2-mediated accumulation of $Ins(1,4,5)P_3$. a, wild-type HEK293 cells (▲) or cells expressing either hNmU-R1 (□) or hNmU-R2 (○) were cultured on 24-well plates and challenged with 10 nM hNmU-25 for the time shown before extraction and determination of $Ins(1,4,5)P_3$ using a radioreceptor assay. Data are mean $\pm$ S.E.M., n = 3. Cells expressing hNmU-R1 (b) or hNmU-R2 (c) were cultured on glass coverslips, transiently transfected with the eGFP-$PH_{PLC\delta1}$ construct, and imaged by confocal microscopy. Cells were challenged with 10 nM hNmU-25 at 15 s. Changes in cytosolic fluorescence [as an index of $Ins(1,4,5)P_3$ levels] were averaged from six cells chosen at random in the field of view but were representative of all cells. Images A, B, and C were taken at the time points indicated on the graphs. Data are representative of at least three separate experiments.

bachol is suggestive of homologous and partial heterologous desensitization that either persists despite agonist removal or alternatively is a consequence of continued signaling by NmU receptors. The latter is consistent with the sustained accumulation of [^{3}H]InsP_x under a Li^+-block in HEK293 cells (see above), suggesting that heterologous desensitization could occur simply through, for example, depletion of a shared intracellular Ca^{2+} store. Together, these data suggest that our wash protocol was not sufficient to remove receptor-bound hNmU-25. To further explore this, we used four complimentary approaches: the influence of washing on the accumulation of [^{3}H]InsP_x, receptor cross-talk, the visualization of NmU binding using a fluorescently labeled NmU, and the ability of excess cold NmU to displace receptor-bound ^{125}I-NmU.

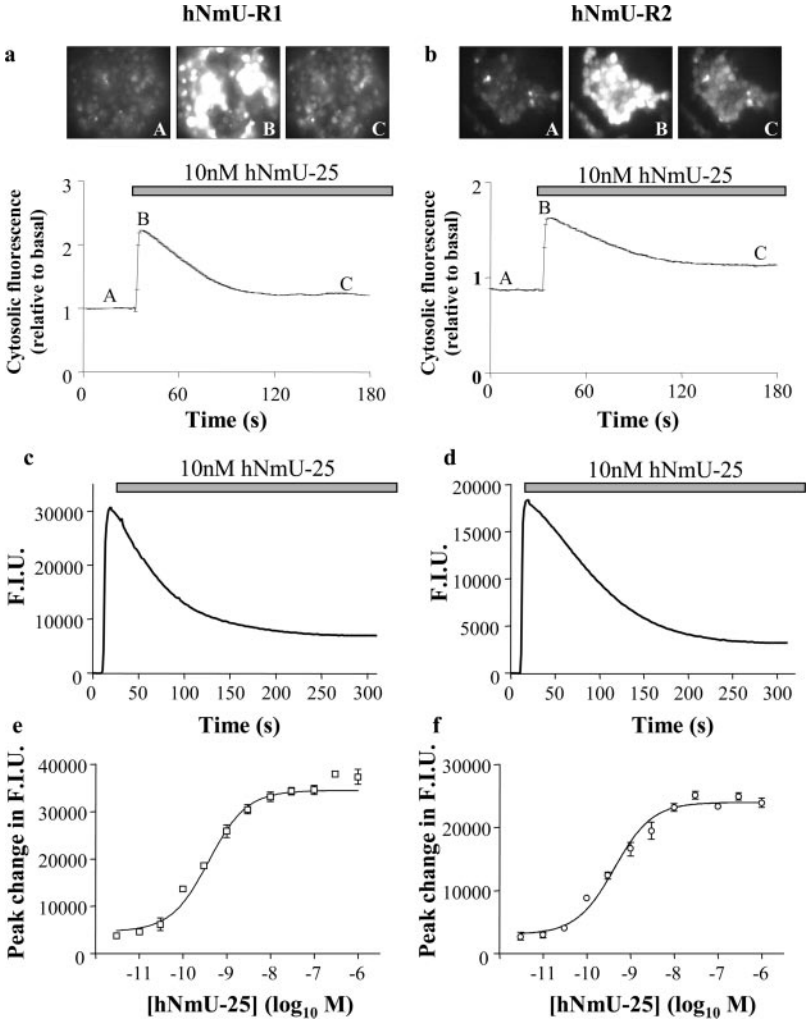

Fig. 4. hNmU-R1- and hNmU-R2-mediated changes in $[Ca^{2+}]_i$. hNmU-R1- (a) or hNmU-R2 (b)-expressing cells were cultured on glass coverslips, loaded with fluo-3-AM, and cytosolic fluorescence was determined by confocal microscopy as an index of $[Ca^{2+}]_i$. Cells were challenged with 10 nM hNmU-25 at 30 s. Traces show the average change in cytosolic fluorescence of six cells in the field of view chosen at random. Images A, B and C were taken at the time points indicated on the traces. Data are representative of at least four separate experiments. c to f, $[Ca^{2+}]_i$ in cell populations was determined using fluo-4-loaded cells and a FLIPR. The time course of 10 nM hNmU-25-mediated changes in fluorescence intensity units (F.I.U) as an index of $[Ca^{2+}]_i$ is shown for cells expressing either hNmU-R1 (c) or hNmU-R2 (d). The concentration-response relationships for hNmU-25-mediated peak elevations of $[Ca^{2+}]_i$ in cells expressing either hNmU-R1 (e) or hNmU-R2 (f) gave pEC_{50} values of 9.41 ± 0.09 and 9.37 ± 0.06, respectively. Data are mean ± S.E.M., $n = 3$.

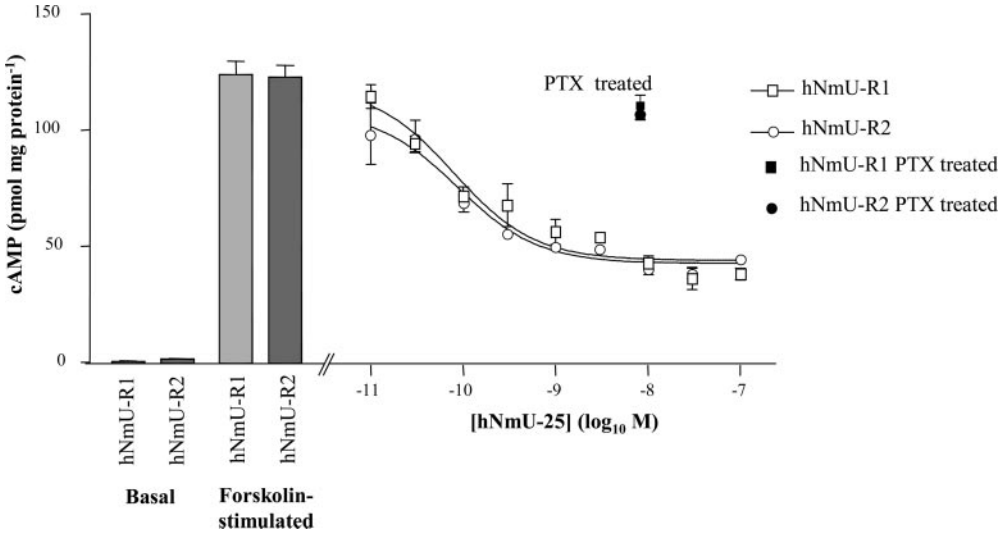

Fig. 5. hNmU-R-mediated inhibition of forskolin-stimulated cAMP accumulation. Cells expressing either hNmU-R1 or hNmU-R2 were cultured on poly-D-lysine-coated 24-well plates. hNmU-25 was added for 10 min before addition of 10 μM forskolin. After a further 10-min incubation, cAMP was extracted and measured by radioreceptor assay. Shown at left are basal and forskolin-stimulated levels of cAMP in cells expressing either hNmU-R1 or hNmU-R2. At right are curves showing the concentration dependence of the hNmU-25-mediated inhibition of forskolin-stimulated cAMP accumulation. The pEC_{50} values for inhibition were 10.10 ± 0.16 for hNmU-R1 (□) and 10.06 ± 0.17 for hNmU-R2 (○). After pertussis toxin treatment of cells (PTX; 20 h; 100 ng/ml), 10 nM hNmU-25 failed to inhibit forskolin-stimulated cAMP accumulation in cells expressing either hNmU-R1 (■) or hNmU-R2 (●). All data are mean + S.E.M., $n = 3$.

The Influence of Washing Cells to Remove hNmU-25 on the Accumulation of [^{3}H]InsP$_x$. As an initial approach to explore the ability to remove receptor-bound hNmU-25, we examined the impact of extensively washing cells during the linear phase of accumulation of [^{3}H]InsP$_x$ under a Li^+ block of inositol monophosphatase. Cells expressing hNmU-R1 were challenged with 10 nM hNmU-25 and after 10 min were either 1) untreated or alternatively, the buffer removed and the cells washed (three times with 1 ml of buffer) before replacement of buffer 2) without or 3) with 10 nM hNmU-25. Irrespective of the manipulation, the rate and extent of accumulation of [^{3}H]InsP$_x$ was similar (Fig. 9a). Identical data were obtained using cells expressing hNmU-R2 (data not shown). This is in contrast to similar manipulations using 100 μM carbachol, where removal of carbachol abolished further accumulation of [^{3}H]InsP$_x$ (Fig. 9b).

Receptor Cross-Talk. As a second approach to examine whether receptor-bound hNmU-25 could be removed with

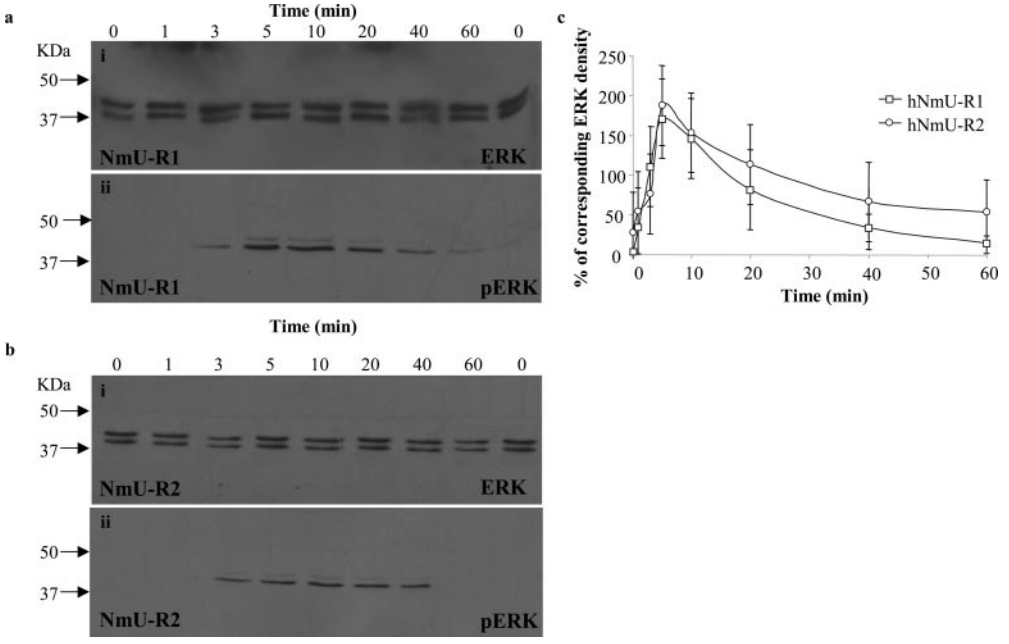

Fig. 6. Activation of ERK by hNmU-R1 or hNmU-R2. Cells expressing either hNmU-R1 (a) or hNmU-R2 (b) were cultured on poly-D-lysine-coated 24-well plates and stimulated with 10 nM hNmU-25 for up to 60 min. Levels of ERK were determined by Western blotting (a, i, hNmU-R1; b, i, hNmU-R2) before being stripped and reprobed for pERK (a, ii, hNmU-R1; b, ii, hNmU-R2). Data are representative of four separate experiments. The density of pERK after stimulation of hNmU-R1 (□) or hNmU-R2 (○) was then related to the corresponding ERK density (c) using a Syngene Genegenius Bioimaging System. Data are mean ± S.E.M., $n = 4$.

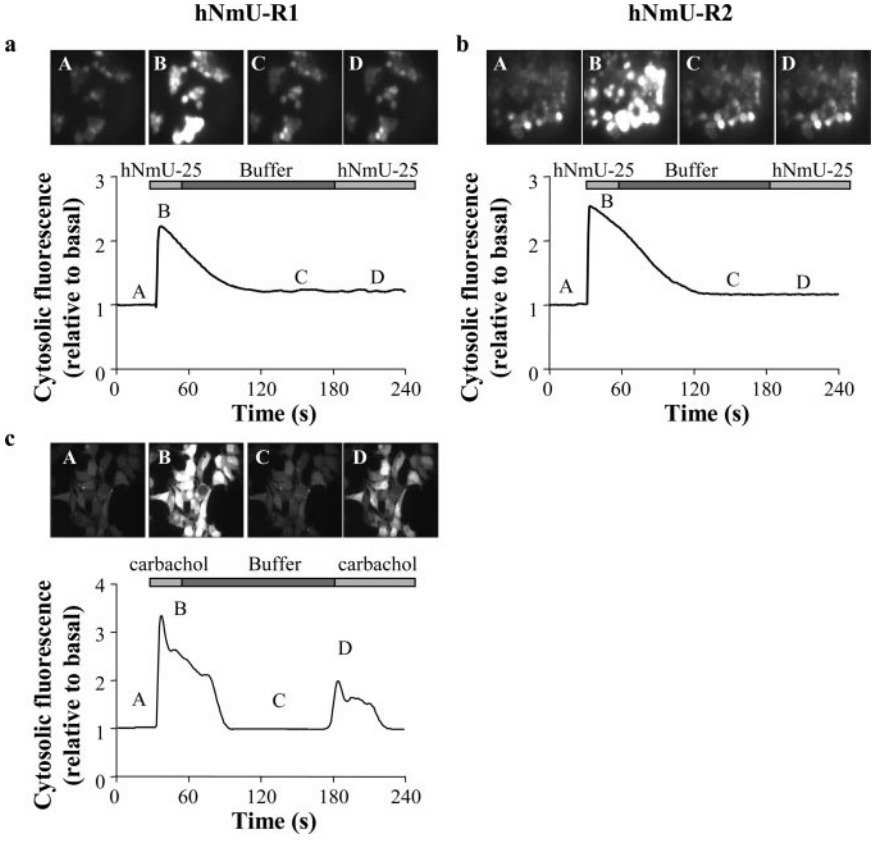

Fig. 7. $[Ca^{2+}]_i$ responses to repeated application of hNmU-25 in cells expressing either hNmU-R1 or hNmU-R2. Cells were cultured on glass coverslips, loaded with fluo-3, and cytosolic fluorescence was measured as an index of $[Ca^{2+}]_i$ using confocal microscopy. Cells expressing either hNmU-R1 (a) or hNmU-R2 (b) were challenged with 10 nM hNmU-25 at 30 s. In c, cells expressing hNmU-R1 were challenged with 100 μM carbachol at 30 s. In each case, cells were perfused at 60 s with agonist-free buffer for a further 120 s. At 180 s, either 10 nM hNmU-25 (a and b) or 100 μM carbachol (c) were reapplied. Changes in cytosolic fluorescence of all cells in the field of view were averaged and expressed relative to basal levels. Images A, B, C, and D, were taken at the time points indicated. Data are representative of at least four experiments.

buffer, we made use of cross-talk between receptors coupled to $G\alpha_{q/11}$ and those coupled to either $G\alpha_s$ or $G\alpha_i$. As a consequence of such cross-talk, after activation of a $G\alpha_{q/11}$-coupled receptor, activation of either a $G\alpha_s$- or $G\alpha_i$-coupled receptor can, in some instances, result in the appearance or potentiation of Ca^{2+} signaling (Werry et al., 2003). Often the ongoing activation of $G\alpha_{q/11}$-coupled receptors is required for the cross-talk, and this has the potential to reveal whether these receptors are active at the time of challenge of $G\alpha_s$- or $G\alpha_i$-coupled receptors. In HEK293 cells, challenge of an endogenous β_2-adrenoceptor with 10 μM noradrenaline did not elevate $[Ca^{2+}]_i$ (Fig. 10a). However, after and in the continued presence of carbachol-mediated activation of the $G\alpha_{q/11}$-coupled muscarinic M_3 receptor, application of 10 μM noradrenaline resulted in a robust elevation of $[Ca^{2+}]_i$ (Fig. 10a). Removal of carbachol by a 2-min wash with KHB abolished the $[Ca^{2+}]_i$ response to a subsequent application of noradrenaline (Fig. 10b), confirming the need for ongoing activation of the $G\alpha_{q/11}$-coupled receptor to mediate receptor cross-talk. Challenge of cells with 10 μM noradrenaline after and in the continued presence of 10 nM hNmU-25 also provoked a robust elevation of $[Ca^{2+}]_i$ in cells expressing hNmU-R1 (Fig. 10c). Washing the cells with KHB for 3 min after challenge with 10 nM hNmU-25 did not abolish the subsequent $[Ca^{2+}]_i$ response to noradrenaline (Fig. 10d), suggesting that hNmU-R1 was still active. Data obtained using cells expressing hNmU-R2 were identical to those obtained using cells expressing hNmU-R1 (data not shown).

Binding of Fluorescently Labeled NmU. As a third approach to determine whether a wash with KHB is sufficient to remove receptor-bound hNmU-25, we used porcine NmU-8 with an N-terminally conjugated fluorophore, Cy3B (NmU-8-Cy3B; 10 nM). In studies based on $[^3H]InsP_x$ accumulation, NmU-8-Cy3B was equipotent with both unlabeled hNmU-25 and porcine NmU-8 (Table 1).

Addition of NmU-8-Cy3B to cells expressing hNmU-R1 resulted in an immediate appearance of intense fluorescence localized to the plasma membrane (Fig. 11a, ii). No fluorescence was observed after an identical addition to wild-type HEK293 cells (data not shown). At 1 min after the addition of NmU-8-Cy3B, the addition of 1 μM hNmU-25 did not result in a loss of plasma membrane fluorescence in hNmU-R1-expressing cells (Fig. 11b, i and ii). Furthermore, after addition of 10 nM NmU-8-Cy3B at 12°C (to block receptor internalization), continuous perfusion of cells with KHB (5 ml/min) did not diminish plasma membrane fluorescence (Fig. 11c, i and ii). Addition of 1 μM hNmU-25 before the addition of NmU-8-Cy3B abolished the appearance of plasma membrane fluorescence in hNmU-R1-expressing cells (Fig. 11d, ii).

Several alternative wash protocols were used in an attempt to remove bound NmU-8-Cy3B (data not shown). These included increasing the salt concentration of the KHB (up to 200 mM NaCl), the addition of acetic acid (up to 50 mM), and reducing the buffer pH with HCl. Only when the buffer was reduced to pH 2.0 was there any loss of plasma membrane fluorescence. The loss of membrane fluorescence was immediate and full. After a return of the cells to buffer at pH 7.4, membrane fluorescence reappeared only after the readdition of NmU-8-Cy3B. This wash and rebinding procedure could be carried out at least three times without any discernible reduction in the fluorescence associated with the membrane in the presence of NmU-8-Cy3B at pH 7.4 (data not shown). However, even in the absence of any prestimulation, this pH 2.0 wash resulted in a marked reduction in both $[Ca^{2+}]_i$ and $[^3H]InsP_x$ responses to either hNmU-25 or carbachol (data not shown). At 37°C (rather than 12°C), addition of NmU-8-Cy3B also resulted in membrane fluorescence (Fig. 11e, i) that could not be removed using KHB. Furthermore, after approximately 5 min (300 s), membrane

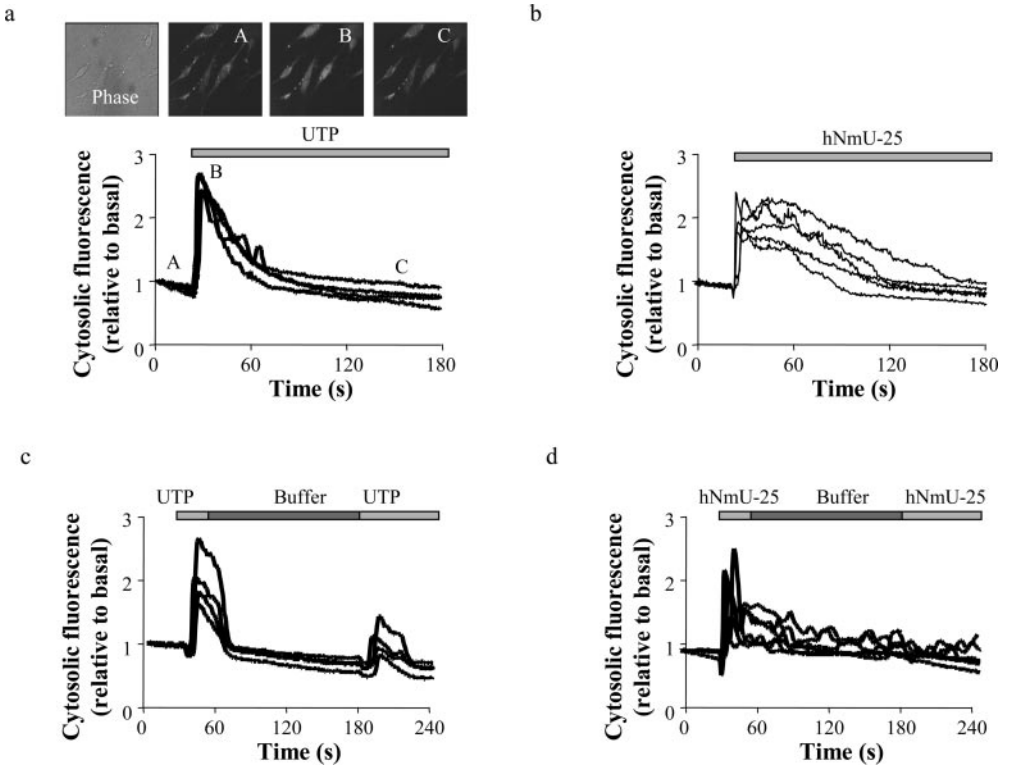

Fig. 8. $[Ca^{2+}]_i$ responses to repeated application of hNmU-25 and UTP in smooth muscle cells isolated from rat fundus. Smooth muscle cells were dissociated from rat stomach fundus and cultured on glass coverslips for 5 days. Cells were loaded with fluo-3 and cytosolic fluorescence measured as an index of $[Ca^{2+}]_i$ using confocal microscopy. Cells were challenged with either 300 μM UTP (a) or 10 nM hNmU-25 (b) at 30 s. In further experiments, naive cells were challenged with either 100 μM UTP (c) or 10 nM hNmU-25 (d) at 30 s, and at 60 s cells were perfused with agonist-free buffer. At 180 s, 300 μM UTP (c) or 10 nM hNmU-25 (d) was reapplied. Changes in the cytosolic fluorescence of three to six cells within the field of view were plotted individually. In a, fluorescent images A, B, and C were taken at the points indicated on the graph. All data are representative of at least three experiments.

fluorescence began to reduce coincident with the appearance of punctate fluorescence within the cell (Fig. 11e, ii), indicating internalization of the ligand. By approximately 8 to 10 min, cellular fluorescence was almost exclusively punctate and cytosolic (Fig. 11e, iii). All experiments with NmU-8-Cy3B were repeated in cells expressing hNmU-R2, and identical results were obtained (data not shown).

Displacement of Prebound ^{125}I-hNmU-25. As a final approach to examine the possible irreversible binding of NmU, we prebound ^{125}I-hNmU-25 to membranes prepared from cells expressing either hNmU-R1 or hNmU-R2. Membranes (10 μg) were incubated for 1 h at room temperature with 150 pM ^{125}I-hNmU-25 to label approximately 50% of the receptors. An excess of unlabeled hNmU-25 (1 μM) was then added, and the amount of ^{125}I-hNmU-25 remaining bound over the next hour was determined. The prebinding of ^{125}I-hNmU-25 resulted in the specific binding of approximately 2600 dpm. The addition of unlabeled hNmU-25 did not reduce the amount of bound ^{125}I-hNmU-25 (100 ± 5% remaining bound after 1 h).

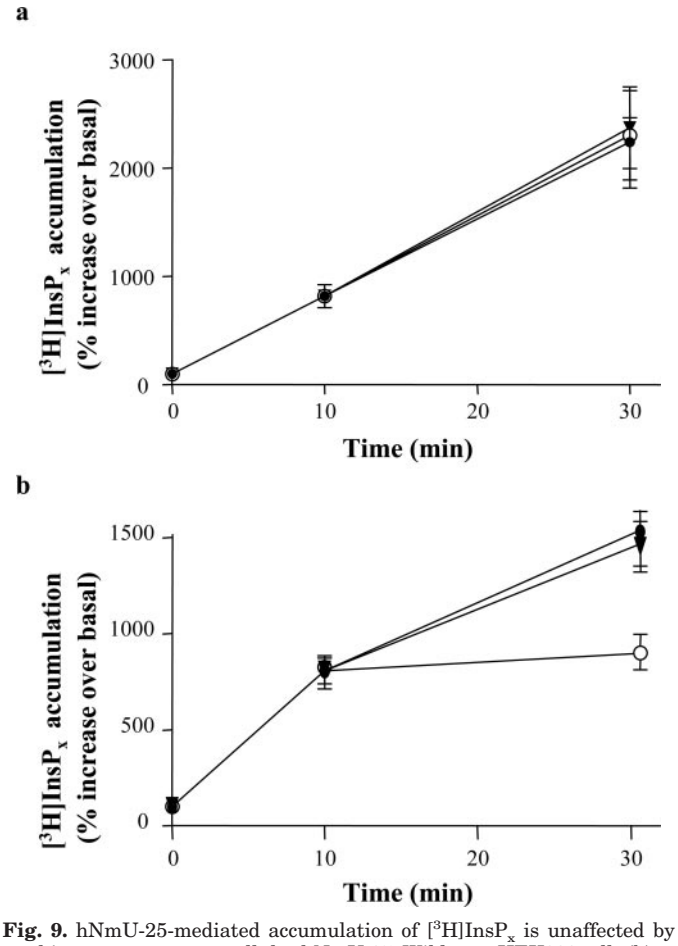

Fig. 9. hNmU-25-mediated accumulation of [^{3}H]InsP$_x$ is unaffected by washing to remove extracellular hNmU-25. Wild-type HEK293 cells (b) or cells expressing hNmU-R1 (a) were cultured in 24-well plates and loaded with [*myo*-^{3}H]inositol for 48 h before challenge with 10 nM hNmU-25 in the presence of a 10 mM Li^+ block of inositol monophosphatase activity. Cells were challenged with 10 nM hNmU-25 (a) or 100 μM carbachol (b) and after 10 min were either untreated (●) or the buffer removed and the cells washed (three times with 1 ml of buffer) before replacement of buffer either without (○) or with (▼) agonist. Data are mean ± S.E.M, $n = 3$.

Discussion

The current study characterizes many aspects of the signaling profiles of the two human receptors for the neuropeptide NmU. Using HEK293 cells with stable expression of either hNmU-R1 or hNmU-R2, we demonstrate coupling to both $G\alpha_{q/11}$ and $G\alpha_i$ G proteins and that activation of these receptors results in robust phosphoinositide and Ca^{2+} signaling and in the inhibition of forskolin-stimulated accumulations of cAMP.

It is clear from the functional screening assays that hNmU-R1 and hNmU-R2 of human and rodent origin are able to mediate intracellular Ca^{2+} signaling with potency in the nanomolar range (Fujii et al., 2000; Hedrick et al., 2000; Hosoya et al., 2000; Howard et al., 2000; Kojima et al., 2000; Raddatz et al., 2000; Shan et al., 2000; Szekeres et al., 2000; Funes et al., 2002). For hNmU-R1, this has been shown to be associated with phosphoinositide hydrolysis (Raddatz et al., 2000; Szekeres et al., 2000). Here, we demonstrate that agonist activation of either hNmU-R1 or hNmU-R2 with hNmU-25 caused accumulations of [^{3}H]InsP$_x$ for at least 1 h against a Li^+ block of inositol monophosphatase activity. Furthermore, studies on cell populations demonstrated rapid, transient elevations of $[Ca^{2+}]_i$ that quickly subsided to small but sustained elevations. hNmU-25-mediated accumulations of [^{3}H]InsP$_x$ and elevations of $[Ca^{2+}]_i$ were potent, each with EC_{50} values of approximately 1 nM for both receptor subtypes. The sustained accumulation of [^{3}H]InsP$_x$ over at least 1 h of agonist stimulation indicates that neither hNmU-R1 nor hNmU-R2 is subject to a rapid and full desensitization. However, closer examination over the first few minutes of stimulation revealed a biphasic accumulation consisting of an initial rapid but transient accumulation followed by a slower but sustained accumulation. This early switch from rapid to slower accumulation indicates a reduction in phospholipase C activity (Wojcikiewicz et al., 1993) consistent with a rapid but partial desensitization of signaling. This pattern is also consistent with a variety of other phospholipase C-coupled receptors (Wojcikiewicz et al., 1993; Willars and Nahorski, 1995). Although the mechanism of desensitization is unclear, an obvious candidate is receptor-G protein uncoupling after agonist-dependent receptor phosphorylation by G protein receptor kinases or second messenger-dependent kinases. Although the level of Ins(1,4,5)P_3 is determined by both its generation and metabolism, the peak and plateau of hNmU-25-mediated increases in this second messenger is also consistent with a rapid but partial desensitization of signaling.

The similarity of the EC_{50} values for both Ins(1,4,5)P_3 accumulation and elevation of $[Ca^{2+}]_i$ are consistent with a tight coupling between these two events. Furthermore, our single cell imaging of $[Ca^{2+}]_i$ in fluo-3-AM-loaded cells and Ins(1,4,5)P_3 using the eGFP-$PH_{PLC\delta1}$ biosensor (Nash et al., 2001) demonstrate that these events are temporally similar and reflective of the average signals generated by the study of cell populations. The initial hNmU-25-mediated Ca^{2+} signaling arises from a thapsigargin-sensitive intracellular store, whereas the sustained component is dependent on a transmembrane $[Ca^{2+}]$ gradient, most likely reflecting capacitative Ca^{2+} entry.

In our initial attempt to examine the potential desensitization of hNmU-25-mediated Ca^{2+} signaling using classic

rechallenge protocols, a second addition of hNmU-25, after an initial challenge and wash, failed to elevate $[Ca^{2+}]_i$. This was also true of NmU-mediated Ca^{2+} signaling in cultured rat fundus smooth muscle cells, suggesting that endogenously expressed receptors behave similarly. Although such behavior could be a consequence of desensitization, this is totally inconsistent with the sustained plateau of $[Ca^{2+}]_i$ elevation in HEK293 cells and smooth muscle cells and the sustained accumulation of $[^3H]InsP_x$ in HEK293 cells. These data suggest that our wash protocol was unable to remove high-affinity hNmU-25 binding to its receptors. This was confirmed for recombinant hNmU-R1 and hNmU-R2 using a variety of approaches, namely, the sustained accumulation of $[^3H]InsP_x$ despite attempts to remove the ligand, the phenomenon of cross-talk between $G\alpha_{q/11}$- and $G\alpha_s$-coupled receptors, the irreversible binding of fluorescently labeled NmU (NmU-8-Cy3B), and the inability of excess hNmU-25 to displace prebound ^{125}I-hNmU-25. Although slightly acidic washes (pH 4–5) are often used to remove peptide ligands, these, as with the endothelin-A receptor (Hilal-Dandan et al., 1997), proved ineffective in the removal of NmU-8-Cy3B from either hNmU-R1 or hNmU-R2. Indeed, only highly acidic washes (≤pH 2) were able to remove NmU-8-Cy3B, and although rebinding was possible, such acidity alone not surprisingly influenced cell signaling, making it impossible to study further the desensitization using rechallenge protocols.

It is interesting that at 37°C, there was a substantial internalization of the fluorescently labeled NmU over relatively short time frames. Given the clear high-affinity binding of NmU, this almost certainly reflects receptor internalization. However, substantial receptor internalization is somewhat in contrast to the sustained linear accumulation of $[^3H]InsP_x$ between 1 and 60 min, even after removal of free hNmU-25 by washing. This suggests that the recycling of receptors and binding of additional hNmU-25 is unlikely to be required for sustained signaling and that sufficient active receptors either remain at the cell surface or are returned (with or without ligand). Further studies are required to distinguish these possibilities. Another possibility is that internalized receptors continue signaling, and although it has been demonstrated that internalized muscarinic receptors cannot contribute to phosphoinositide turnover (Sorenson et al., 1997), whether this is true of all receptors in all circumstances is essentially unknown. As with many other peptide ligands, such as endothelin A (Hilal-Dandan et al., 1997) and substance P (Schmidlin et al., 2001), the irreversible interaction of hNmU-25 with its receptors has implications on the function and regulation of its receptors. The physiological consequence of irreversible binding is unclear but may limit the responsiveness of the receptors to repeat agonist challenge.

GPCR-mediated activation of MAP kinase by both recombinant and endogenous receptors is well documented but mechanistically complex (Belcheva and Coscia, 2002). In this

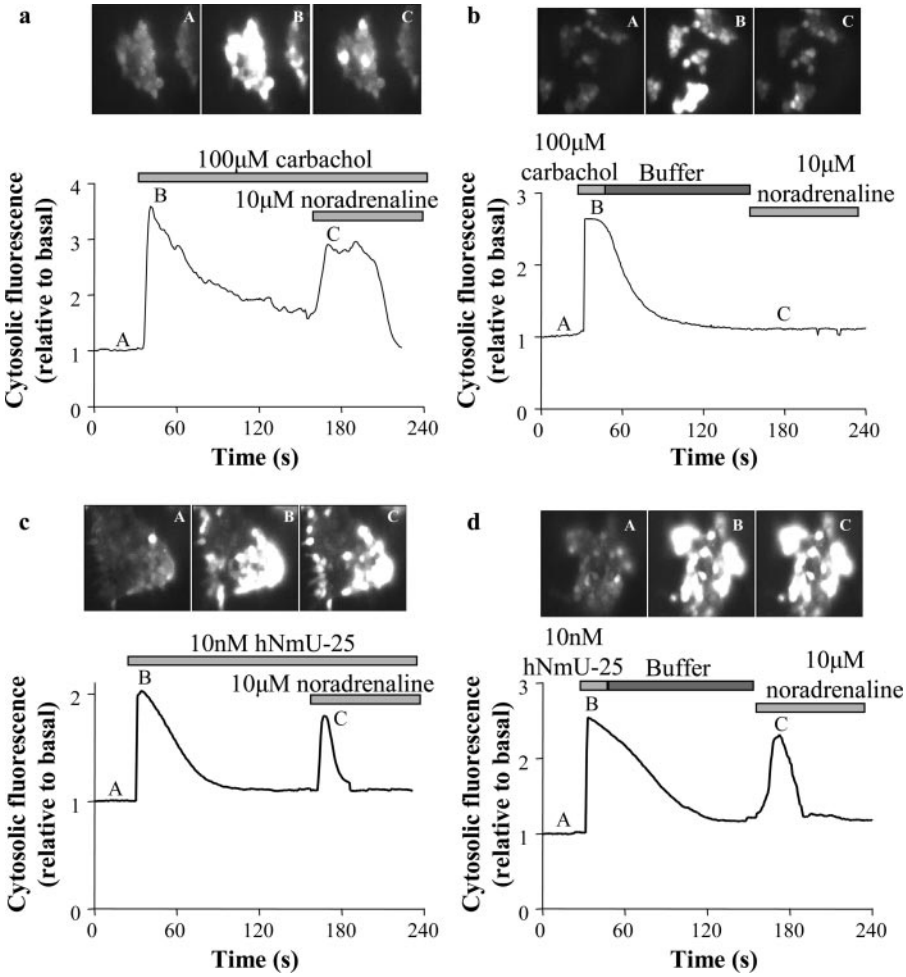

Fig. 10. Cross-talk between receptors resulting in enhanced $[Ca^{2+}]_i$ signaling. Cells were cultured on glass coverslips, loaded with fluo-3, and cytosolic fluorescence was measured as an index of $[Ca^{2+}]_i$ using confocal microscopy. Wild-type HEK293 cells were challenged with 100 μM carbachol at 30 s to activate endogenous $G\alpha_q$-coupled muscarinic-M_3 receptors, followed by 10 μM noradrenaline at 150 s to activate endogenous $G\alpha_s$-coupled β_2-adrenoceptors. Noradrenaline was applied either in the continued presence of carbachol (a) or after a 120-s wash with buffer (b). HEK293 cells expressing hNmU-R1 were challenged with 10 nM hNmU-25 at 30 s followed by 10 μM noradrenaline either in the continued presence of hNmU-25 (c) or after a 120-s wash with buffer (d). Changes in cytosolic fluorescence of all cells in the field of view were averaged and expressed relative to basal levels. All experiments are representative of three experiments. The experiments in c and d were repeated using cells expressing hNmU-R2 and similar data were obtained (not shown).

report, we show that hNmU-25-mediated activation of ERK is pertussis toxin-insensitive, suggesting that $G\alpha_{q/11}$ coupling to phosphoinositide and Ca^{2+} signaling may be responsible. This is consistent with a variety of other receptors (Belcheva and Coscia, 2002). For some GPCRs (Daaka et al., 1998) but not all (Budd et al., 1999), internalization seems to be a requirement for activation of MAP kinase. Although our data indicate rapid internalization of both hNmU-R1 and hNmU-R2 within 4 to 5 min of addition, the consequence of this internalization in the activation and regulation of signaling pathways, including the MAP kinase pathway remains to be established.

hNmU-25-mediated accumulation of $[^3H]InsP_x$ by either hNmU-R1 or R2 is also insensitive to pertussis toxin, demonstrating a lack of involvement of $G\alpha_{i/o}$ in this response. This is consistent with the pertussis toxin-insensitive Ca^{2+} signaling by both hNmU-R1 and hNmU-R2 (Raddatz et al., 2000; Shan et al., 2000; Szekeres et al., 2000) and indicates a $G\alpha_{q/11}$-mediated activation of phospholipase C. The direct coupling of both receptors to $G\alpha_{q/11}$ was confirmed by showing an hNmU-25 dependent increase in binding of $[^{35}S]GTP\gamma S$ to this G protein. These studies also demonstrated activation of $G\alpha_i$ by both receptors. Potential differences in the ability of antibodies to immunoprecipitate the different G protein α-subunits means that we are unable to directly compare the levels of $G\alpha_{q/11}$ and $G\alpha_i$ activation. However, both receptor subtypes were able to inhibit forskolin-stimulated cAMP accumulation, thereby demonstrating functional relevance of $G\alpha_i$ activation. The coupling of GPCRs to multiple G proteins has, of course, been reported previously (for review, see Hermans, 2003). Although the promiscuous coupling of GPCRs to G proteins can be the consequence of aspects such as high-receptor expression levels or the agonist used, such promiscuity seems to be a physiological reality for a number of receptors (Hermans, 2003). In our studies, we were also able to show the activation of $G\alpha_i$ using the immunoprecipitation protocol in membranes from additional hNmU-R clonal cell lines that expressed lower levels of receptor. Furthermore, both hNmU-R1 and hNmU-R2 inhibited forskolin-stimulated cAMP accumulation more potently than the elevation of Ca^{2+} or accumulation of $[^3H]InsP_x$, again suggesting that this coupling may not be simply a consequence of high levels of receptor expression. It has been reported previously that hNmU-25 partially inhibits forskolin-stimulated cAMP accumulation in Chinese hamster ovary cells with stable expression of hNmU-R2 (Hosoya et al., 2000), whereas activation of transiently expressed hNmU-R1 in HEK293 cells has no affect on

TABLE 1

Comparative pEC_{50} values of porcine NmU-8-Cy3B, human NmU-25, and porcine NmU-8 for $[^3H]InsP_x$ accumulation mediated by recombinantly expressed hNmU-R1 or hNmU-R2

Agonist	hNmU-R1	hNmU-R2
Human NmU-25	9.14 ± 0.07	8.97 ± 0.18
Porcine NmU-8	8.81 ± 0.09	8.70 ± 0.05
Porcine NmU-8-Cy3B	8.88 ± 0.09	8.79 ± 0.06

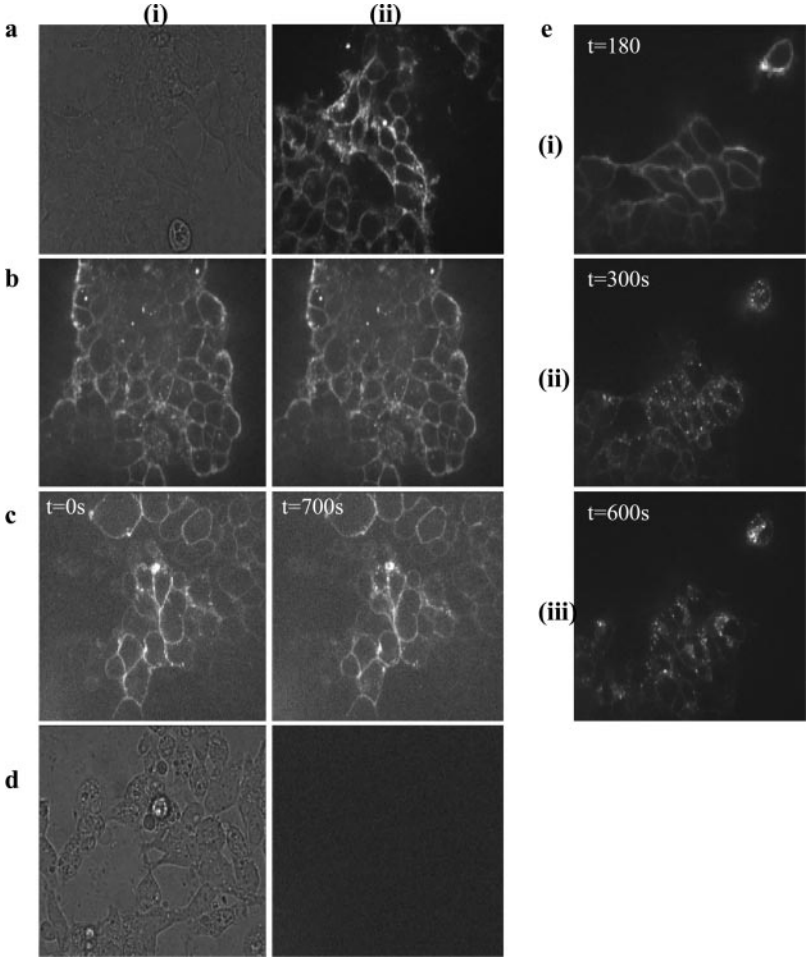

Fig. 11. Binding of fluorescently-tagged NmU-8 to cells expressing hNmU-R1. Cells expressing hNmU-R1 were cultured on glass coverslips and imaged using confocal microscopy. Phase image (a, i) and fluorescence image (a, ii) of cells after addition of 10 nM NmU-8-Cy3B. Fluorescence image of cells after addition of 10 nM NmU-8-Cy3B (b, i) and the same cells after addition of 1 μM hNmU-25 (b, ii). NmU-8-Cy3B (10 nM) was added to cells at 0 s (c, i), and the cells were then perfused with buffer (5 ml/min) for 700s (c, ii) at 12°C. Phase image (d, i) and fluorescence image (d, ii) of cells that were exposed to 10 nM NmU-8-Cy3B after addition of (and in the continued presence of) 1 μM hNmU-25. Fluorescence image of NmU-8-Cy3B at 37°C, at either 180 s (e, i), 300 s (e, ii), or 600 s (e, iii). All images are representative of at least three separate experiments. Identical experiments were performed using cells expressing hNmU-R2 with identical results (data not shown).

either the basal or forskolin-stimulated levels of cAMP (Szekeres et al., 2000). Whether this dual coupling is true of any endogenously expressed hNmU receptors, and its physiological and therapeutic relevance, remains to be established.

In summary, we have shown that activation of human NmU receptors recombinantly expressed in HEK293 cells results in the activation of both phospholipase C and inhibition of adenylyl cyclase as demonstrated by increases in $[Ca^{2+}]_i$, $Ins(1,4,5)P_3$, and $[^3H]InsP_x$ accumulation and by a reduction in forskolin-elevated cAMP, respectively. Furthermore, by directly assessing the coupling of G proteins, we have demonstrated that the activation of these pathways is the result of the dual coupling to both $G\alpha_{q/11}$ and $G\alpha_i$ G proteins, whereas, consistent with a lack of increase in basal levels of cAMP upon receptor activation, no coupling is observed to $G\alpha_s$. We have also demonstrated that both hNmU-R1 and R2 activate MAP kinase. Finally, our data clearly demonstrate that NmU binding is of high affinity and that it binds essentially irreversibly under physiological conditions and that this binding is followed rapidly by internalization. Despite structural differences between the two hNmU receptor subtypes, these studies have not revealed differences in the signaling properties of these two receptor types.

Acknowledgments

We thank J. Scott and M. Ruediger (GlaxoSmithKline) for the generation and purification of Cy3B-NmU-8. We also thank both E. Appelbaum and E. Dul (GEPB, Upper Merion, Philadelphia, PA) for generating the stable cell lines and N. Elshourbagy and U. Shabon (Gene Cloning and Expression Proteomics, GlaxoSmithKline) for cloning the receptors. We also thank S. Ratcliffe (GlaxoSmithKline) for supplying hNmU-25 and F. McKay (GlaxoSmithKline) for help in using the FLIPR.

References

Aiyar N, Baker E, Wu HL, Nambi P, Edwards RM, Trill JJ, Ellis C, and Bergma DL (1994) Human AT_1 receptor is a single-copy gene-characterization in a stable cell-line. *Mol Cell Biochem* **131:**75–86.

Akam EC, Challiss RAJ, and Nahorski SR (2001) $G_{q/11}$ and $G_{i/o}$ activation profiles in CHO cells expressing human muscarinic acetylcholine receptors: dependence on agonist as well as receptor-subtype. *Br J Pharmacol* **132:**950–958.

Augood SJ, Keast JR, and Emson PC (1988) Distribution and characterization of neuromedin-U-like immunoreactivity in rat-brain and intestine and in guinea-pig intestine. *Regul Peptides* **20:**281–292.

Belcheva MM and Coscia CJ (2002) Diversity of G-protein-coupled receptor signaling pathways to ERK/MAP kinase. *Neurosignals* **11:**34–44.

Bockman CS, Abel PW, Hicks JW, and Conlon JM (1989) Evidence that neuromedin-U may regulate gut motility in reptiles but not in mammals. *Eur J Pharmacol* **171:**255–257.

Brighton PJ, Szekeres PG, and Willars GB (2004) Neuromedin U and its receptors: structure, function and physiological roles. *Pharmacol Rev* **56:**231–248.

Brown BL, Albano JDM, Ekins RP, Sgherzi AM, and Tampion W (1971) A simple and sensitive saturation assay method for the measurement of adenosine 3′5′-cyclic monophosphate. *Biochem J* **121:**561–562.

Budd DC, Rae A, and Tobin AB (1999) Activation of the mitogen-activated protein kinase pathway by a $G_{q/11}$-coupled muscarinic receptor is independent of receptor internalization. *J Biol Chem* **274:**12355–12360.

Bundey RA and Nahorski SR (2001) Homologous and heterologous uncoupling of muscarinic M_3 and α_{1B} adrenoceptors to G $\alpha_{q/11}$ in SH-SY5Y human neuroblastoma cells. *Br J Pharmacol* **134:**257–264.

Chu CP, Jin QH, Kunitake T, Kato K, Nabekura T, Nakazato M, Kanagawa K, and Kannan H (2002) Cardiovascular actions of central neuromedin U in conscious rats. *Regul Peptides* **105:**29–34.

Daaka Y, Luttrell LM, Ahn S, Della Rocca GJ, Ferguson SSG, Caron MG, and Lefkowitz RJ (1998) Essential role for G-protein coupled receptor endocytosis in the activation of MAP kinase. *J Biol Chem* **273:**685–688.

Domin J, Ghatei MA, Chohan P, and Bloom SR (1986) Characterization of neuromedin-U like immunoreactivity in rat, porcine guinea-pig and human-tissue extracts using a specific radioimmunoassay. *Biochem Biophys Res Commun* **140:**1127–1134.

Domin J, Ghatei MA, Chohan P, and Bloom SR (1987) Neuromedin U – a study of its distribution in the rat. *Peptides* **8:**779–784.

Fujii R, Hosoya M, Fukusumi S, Kawamata Y, Habata Y, Hinuma S, Onda H, Nishimura O, and Fujino M (2000) Identification of neuromedin U as the cognate ligand of the orphan G-protein-coupled receptor FM-3. *J Biol Chem* **275:**21068–21074.

Funes S, Hedrick JA, Yang SJ, Shan LX, Bayne M, Monsma FJ, and Gustafson EL (2002) Cloning and characterization of murine neuromedin U receptors. *Peptides* **23:**1607–1615.

Gardiner SM, Compton AM, Bennett T, Domin J, and Bloom SR (1990) Regional hemodynamic-effects of neuromedin-U in conscious rats. *Am J Physiol* **258:**R32–R38.

Hedrick JA, Morse K, Shan LX, Qiao XD, Pang L, Wang S, Laz T, Gustafson EL, Bayne M, and Monsma FJ (2000) Identification of a human gastrointestinal tract and immune system receptor for the peptide neuromedin U. *Mol Pharmacol* **58:**870–875.

Hermans E (2003) Biochemical and pharmacological control of the multiplicity of coupling at G-protein-coupled receptors. *Pharmacol Ther* **99:**25–44.

Hilal-Dandan R, Villegas S, Gonzalez A, and Brunton LL (1997) The quasi-irreversible nature of endothelin binding and G-protein-linked signaling in cardiac myocytes. *J Pharmacol Exp Ther* **281:**267–273.

Hosoya M, Moriya T, Kawamata Y, Ohkubo S, Fujii R, Matsui H, Shintani Y, Fukusumi S, Habata Y, Hinuma S, et al. (2000) Identification and functional characterization of a novel subtype of neuromedin U receptor. *J Biol Chem* **275:**29528–29532.

Howard AD, Wang RP, Pong SS, Mellin TN, Strack A, Guan XM, Zeng ZZ, Williams DL, Feighner SD, Nunes CN, et al. (2000) Identification of receptors for neuromedin U and its role in feeding. *Nature (Lond)* **406:**70–74.

Ivanov TR, Lawrence CB, Stanley PJ, and Luckman SM (2002) Evaluation of neuromedin U actions in energy homeostasis and pituitary function. *Endocrinology* **143:**3813–3821.

Kojima M, Haruno R, Nakazato M, Date Y, Murakami N, Hanada R, Matsuo H, and Kangawa K (2000) Purification and identification of neuromedin U as an endogenous ligand for an orphan receptor GPR66 (FM3). *Biochem Biophys Res Commun* **276:**435–438.

Maggi CA, Patacchini R, Giuliani S, Turini D, Barbanti G, Rovero P, and Meli A (1990) Motor response of the human isolated small-intestine and urinary-bladder to porcine neuromedin U-8. *Br J Pharmacol* **99:**186–188.

Malendowicz KA, Nussdorfer GG, Nowak KW, and Mazzocchi G (1993) Effects of neuromedin U-8 on the rat pituitary-adrenocortical axis. *In Vivo* **7:**419–422.

Minamino N, Kangawa K, and Matsuo H (1985) Neuromedin U-8 and U-25: novel uterus stimulating and hypertensive peptides identified in porcine spinal cord. *Biochem Biophys Res Commun* **130:**1078–1085.

Nakazato M, Hanada R, Murakami N, Date Y, Mondal MS, Kojima M, Yoshimatsu H, Kangawa K, and Matsukura S (2000) Central effects of neuromedin U in the regulation of energy homeostasis. *Biochem Biophys Res Commun* **277:**191–194.

Nash MS, Young KW, Willars GB, Challiss RAJ, and Nahorski SR (2001) Single cell imaging of graded $Ins(1,4,5)P_3$ production following G-protein-coupled receptor activation. *Biochem J* **356:**137–142.

Quayle JM, Dart C, and Standen NB (1996) The properties and distribution of inward rectifier potassium currents in pig coronary arterial smooth muscle. *J Physiol (Lond)* **494:**715–726.

Raddatz R, Wilson AE, Artymyshyn R, Bonini JA, Borowsky B, Boteju LW, Zhou SQ, Kouranova EV, Nagorny R, Guevarra MS, et al. (2000) Identification and characterization of two neuromedin U receptors differentially expressed in peripheral tissues and the central nervous system. *J Biol Chem* **275:**32452–32459.

Schmidlin F, Dery O, DeFea KO, Slice L, Patierno S, Sternini C, Grady EF, and Bunnett NW (2001) Dynamin and rab5a-dependent trafficking and signaling of the neurokinin 1 receptor. *J Biol Chem* **276:**25427–25437.

Shan LX, Qiao XD, Crona JH, Behan J, Wang S, Laz T, Bayne M, Gustafson EL, Monsma FJ, and Hedrick JA (2000) Identification of a novel neuromedin U receptor subtype expressed in the central nervous system. *J Biol Chem* **275:**39482–39486.

Sorenson SD, McEwan EL, Linseman DA, and Fisher SK (1997) Agonist-induced endocytosis of muscarinic cholinergic receptors: relationship to stimulated phosphoinositide turnover. *J Neurochem* **86:**1473–1483.

Szekeres PG, Muir AI, Spinage LD, Miller JE, Butler SI, Smith A, Rennie GI, Murdock PR, Fitzgerald LR, Wu HL, et al. (2000) Neuromedin U is a potent agonist at the orphan G-protein-coupled receptor FM3. *J Biol Chem* **275:**20247–20250.

Westfall TD, McCafferty GP, Pullen M, Gruver S, Sulpizio AC, Aiyar VN, Disa J, Contino LC, Mannan IJ, and Hieble JP (2001) Characterisation of neuromedin U effects in canine smooth-muscle. *J Pharmacol Exp Ther* **301:**987–992.

Werry TD, Christie MI, Dainty IA, Wilkinson GF, and Willars GB (2002) Ca^{2+} signalling by recombinant human CXCR2 chemokine receptors is potentiated by P2Y nucleotide receptors in HEK cells. *Br J Pharmacol* **135:**1199–1208.

Werry TD, Wilkinson GF, and Willars GB (2003) Mechanisms of cross-talk between G-protein-coupled receptors resulting in enhanced release of intracellular Ca^{2+} *Biochem J* **374:**281–296.

Willars GB and Nahorski SR (1995) Quantitative comparisons of muscarinic and bradykinin receptor-mediated $Ins(1,4,5)P_3$ accumulation and Ca^{2+} signalling in human neuroblastoma cells. *Br J Pharmacol* **114:**1133–1142.

Wojcikiewicz RJH, Tobin AB, and Nahorski SR (1993) Desensitization of cell signalling mediated by phosphoinositidase-C. *Trends Pharmacol Sci* **14:**279–285.

Wren AM, Small CJ, Abbott CR, Jethwa PH, Kennedy AR, Murphy KG, Stanley SA, Zollner AN, Ghatei MA, and Bloom SR (2002) Hypothalamic actions of neuromedin U. *Endocrinology* **143:**4227–4234.

Address correspondence to: Dr. Gary. B. Willars, Department of Cell Physiology and Pharmacology, Medical Sciences Building, University of Leicester, University Rd., LE1 9HN UK. E-mail: gbw2@le.ac.uk